We extend our sincere gratitude to the reviewer's valuable guidance provided throughout the review process, which have significantly contributed to the paper's quality. Our responses are listed below, presented in red, following the reviewers' comments, which are in black. The revisions made to the manuscript are highlighted in yellow.

Zhong and colleagues present measurements and detailed analysis using constrained box model approaches of in-situ ozone formation at a field site in the PRD, using a newly-developed direct measurement of ozone production rates, alongside measurements of various atmospheric chemical species/photochemical parameters.

The paper presents an extensive exploration of the measurements, assessing the NOx- and VOC-dependence of the measured and modelled ozone formation, and relating this to (e.g.) missing VOC species. The approach is logical and largely well described (although I have some significant suggestions for clarifications — below), and the work represents a good advance in approaches to analysis of these new measurement approaches/data and could make a valuable contribution; in particular the assessment of ozone production "gaps" vs model with co-reactant concentrations/conditions (NOx/VOC sensitivity)

My principal concern is that the degree of accuracy (and maybe precision) of the measurements may be overestimated, and that the analysis of these – still relatively new – measurements is taken further than the data uncertainties really justify; that the data are over-interpreted.

Thank you for your suggestion. We have thoroughly discussed the measurement accuracy and uncertainties of the custom-made net O₃ production rate (NPOPR) detection system in our previous studies (Hao et al., 2023; Zhou et al., 2024b), and found that the measurement accuracy of the NPOPR detection system is determined as 13.9 %, this is estimated from the systematic errors inherent in the system representing the maximum systematic error resulting from photochemical O₃ production in the reference chamber.

These errors arise from photochemical O₃ productions in the reference chamber, because of the UV protection Ultem film that only filters out the sunlight with wavelengths less than 390 nm. Consequently, photochemical O₃ production from sunlight wavelengths between 390 nm and 790 nm still exist in the reference chamber and causes the systemic errors mentioned above.

Furthermore, according to the $P(O_3)_{\text{net}}$ evaluation method listed in Eq. (5) in the main text, the measurement error of $P(O_3)_{\text{net}}$ depends on the estimation error of Ox in the reaction and reference chambers, which includes the measurement error of O_X of CAPS-NO₂ monitor and the error caused by the light-enhanced loss of O₃. These collective measurement error of $P(O_3)_{\text{net}}$ is referred to as the measurement precision of the NPOPR detection system, which is different with the measurement accuracy described above. This error refers to the degree of consistency or repeatability observed in a set of measurements by the NPOPR detection system. To make the description clearer, we have added this explanation in lines 127- 137 in the main text:

"The mean residence time in the reaction chamber is 0.15 h at the air flow rate of 2.1 L min⁻¹, and the limit of detection (LOD) of the NPOPR detection system is 0.86 ppbv h⁻¹ at the sampling air flow rate of 2.1 L min⁻¹, which is obtained as three times the measurement error of $P(O_3)_{net}$ (Hao et al., 2023). The measurement error of $P(O_3)_{net}$ is determined by the uncertainty in the Ox mixing ratio estimated for both the reaction and reference chambers. This uncertainty combines (i) the measurement uncertainty of the CAPS-NO₂ monitor used to derive Ox and (ii) the error induced by light-enhanced O₃ loss inside the chambers. Taken together, these contributions define the measurement precision of the NPOPR detection system. In addition, the measurement accuracy of the NPOPR detection system is 13.9 %, corresponding to the maximum systematic error arising from photochemical O₃ production in the reference chamber (Hao et al., 2023; Zhou et al., 2024b); details are given in Sect. S1 in the supplementary materials."

And S1 in the supplementary materials:

"S1. Measurement error of P(O3)net of the NPOPR detection system

We have thoroughly described the measurement error of $P(O_3)_{net}$ of the NPOPR detection system in our previous study (Hao et al., 2023; Zhou et al., 2024b). The measurement error of $P(O_3)_{net}$ depends on the estimation error of Ox in the reaction and reference chambers, which includes the measurement error of O_X of CAPS-NO₂ monitor and the error caused by the light-enhanced loss coefficient of $O_3(\gamma)$,

which can be calculated as follows:

$$\left(O_{X}\right)_{\text{error}} = \sqrt{\left(O_{X\gamma}\right)_{\text{error}}^{2} + \left(O_{X_{CAPS}}\right)_{\text{error}}^{2}}$$
(S1)

where $(O_X)_{error}$ represents the absolute error in the estimated O_X concentration in the reaction and reference chambers, which results from the quadratic propogation of the absolute errors $(O_{X_{\gamma}})_{error}$ and $(O_{X_{CAPS}})_{error}$. Here, $(O_{X_{CAPS}})_{error}$ signifies the measurement error of the O_X measured by the CAPS-NO₂ monitor, while $(O_{X_{\gamma}})_{error}$ denotes the error associated with the γ -corrected Ox of the chambers, where γ represent the light-enhanced O_3 loss coefficient.

To get $(O_{X_{CAPS}})_{error}$, we calibrated the CAPS-NO₂ monitor as follows: a. injected ~10–100 ppbv of NO₂ for 30 minutes to passivate the surfaces of the monitor and then injecting ultrapure air for ~ 10 minutes to ensure the zero point did not drift, according to the ultrapure air condition, the LOD of CAPS was 0.88 and 0.02 ppbv (3 σ) at an integration time of 35 and 100 s, respectively; b. injected a wide range of NO₂ concentration (from 0–160 ppbv) prepared from a NO₂ standard gas (with the original concentration of 2.08 ppmv) mixed with ultrapure air into the CAPS-NO₂ monitor, repeated the experiments for three times at each NO₂ concentration, the final results are shown in Fig. S16.

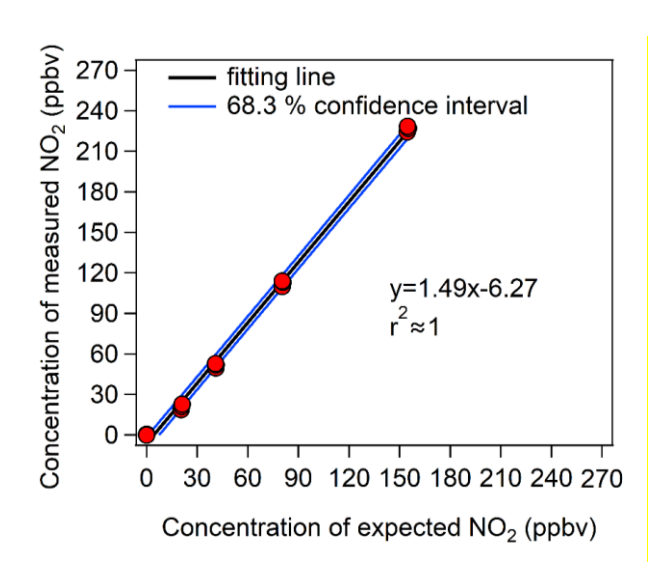


Figure S16: Calibration results of the CAPS NO₂ monitor at different NO₂ mixing ratios. The y-axis represents the NO₂ mixing ratios measured by the CAPS NO₂ monitor, and the x-axis represents the prepared NO₂ mixing ratios prepared from the diluted NO₂ standard gas.

We fitted the calibration results with a 68.3 % confidence level, and the blue line in Fig. S16 represents the maximum fluctuation range under this confidence level, $(O_{X_{CAPS}})_{error}$ was then calculated from the fluctuation range of the 68.3 % confidence interval of the calibration curve, the relationship between the $(O_{X_{CAPS}})_{error}$ and the measured Ox value ([Ox]_{measured}) can be expressed as a power function curve, as shown in Eq. (S2):

$$(O_{X_{CAPS}})_{error} = 9.72 \times [0x]_{measured}^{-1.0024}$$
 (S2)

We acknowledge that this power function has been derived from calibration data of the O_X concentrations

ranged from 20 ppbv to 160 ppbv. Utilizing this function outside this calibrated range, especially at very low O_X concentrations, may result in errors that are disproportionately large and may not accurately capture the true variability of the measurement errors. In this study, the O_X concentrations ranged from 18 to 148 ppbv, which falls into the calibration range. Consequently, this power function is deemed appropriate for estimating the $(O_{X_{CAPS}})_{error}$ throughout the whole measurement period.

 $(O_{X\gamma})_{error}$ was derived from the light-enhanced loss of O_3 in the reaction and reference chambers at 2.1 L min⁻¹, the flow rate used during the observation campaign. To establish the calibration curve, we performed an outdoor experiment: O_3 (~ 130 ppbv), produced by an O_3 generator (P/N 97-0067-02, Analytic Jena US, USA), was induced into the two chambers. Zero air was co-injected with the O_3 to suppress any photochemical O_3 production outdoors. This setup allowed us to monitor daytime changes in the photolysis frequencies of various species. We simultaneously recorded $J(O^1D)$, T, RH, P and O_3 mixing ratios at the inlets and outlets of both chambers. T and RH were measured with a thermometer (Vaisala, HMP110, USA). The light-enhanced O_3 loss coefficient (γ) was then calculated using Eq. (S3):

$$\gamma = \frac{d[O_3] \times D}{\omega \times [O_3] \times \tau} \tag{S3}$$

where $d[O_3]$ represents the difference between the O_3 mixing ratios at the inlets and outlets of both chambers (i.e., the light-enhanced O_3 loss); D is the diameter of the chambers; ω is the average velocity of O_3 molecules; $[O_3]$ is the injected O_3 mixing ratio at the inlet; τ is the average residence time of the air in the reaction and reference chambers. The relationship between $J(O^1D)$ and γ is shown in Fig. S18, the obtained γ - $J(O^1D)$ equation was used to correct $d[O_3]$ in both chambers during the daytime, thereby eliminating the influence of light-enhanced loss. Our previous study has shown that after this correction, $d[O_3]$ showed no clear correlation with RH for either chamber (Hao et al., 2023), indicating that RH did not affect the O_3 mixing ratio during the observation period. When quantifying $d[O_3]$ from ambient air measurements, we first calculate γ from the measured $J(O^1D)$ using the γ - $J(O^1D)$ equations listed in Fig. S17 for each chamber, then compute $d[O_3]$ from the measured $[O_3]$ and Eq. (S3).

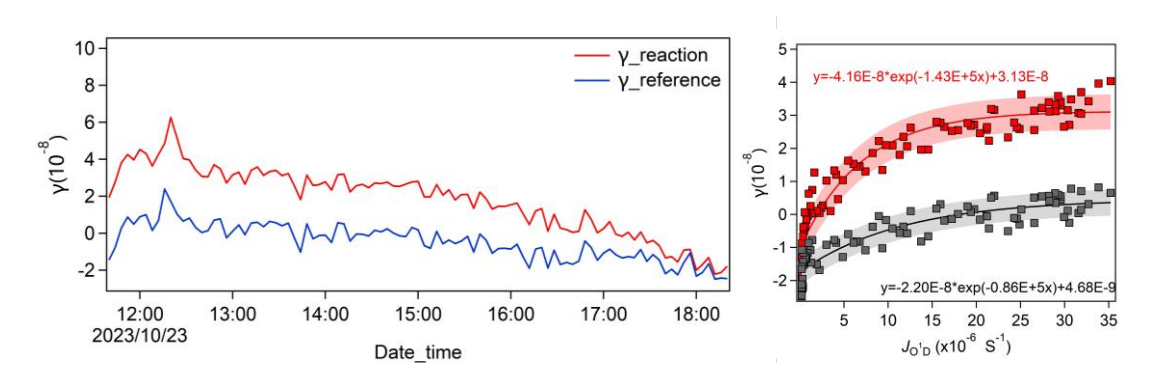


Figure S17: The relationship between γ and $J(O^1D)$ in the reaction and reference chambers, the shaded areas represent the maximum range of fluctuation under this confidence level.

When injecting ambient air into the NPOPR system, the error of $P(O_3)_{net}$ with a residence time of τ can be calculated using Eq. (S4):

$$P(O_3)_{\text{net_error}} = \frac{(O_{X\gamma})_{\text{rea_error}}^2 + ((9.72 \times [(O_X]_{\text{rea_measured}})_{\text{rea_std}}^2) + (O_{X\gamma})_{\text{ref_error}}^2 + ((9.72 \times [(O_X]_{\text{ref_measured}})_{\text{ref_std}}^2))^2}{\tau}$$

$$(S4)$$

where $(O_{X_{\gamma}})_{\text{rea error}}$ and $(O_{X_{\gamma}})_{\text{ref error}}$ represent the measurement error due to light-enhanced loss of O_3 in the reaction and reference chambers, respectively, and $(9.72 \times [O_X]_{\text{measured}}^{-1.0024})_{\text{rea_std}}$ and $(9.72 \times [O_X]_{\text{measured}}^{-1.0024})_{\text{ref_std}}$ represent the standard deviation of O_X in the reaction and reference chambers, respectively, caused by the CAPS NO_2 monitor with an integration time period of 100 s. Combined with the associated residence time $\langle \tau \rangle$ under different flow rates, i.e., $\langle \tau \rangle$ was 0.16 h at a flow rate of 2.1 L min^{-1} . In our previous research (Hao et al., 2023), we evaluated the residence time error and determined it to be approximately 0.0015, when we considered this error in the calculation of ${}^{\circ}P(O_3)_{\text{net}}$ error', we observed a minimal reduction in the ${}^{\circ}P(O_3)_{\text{net}}$ error' values, ranging from 0 to 4% [0.25-0.75 percentile]. This impact is considered negligible in relation to the overall ${}^{\circ}P(O_3)_{\text{net}}$ error' as presented in Eq. S4. Consequently, we did not consider the uncertainty associated with the residence time in our calculations. We note that this collective measurement error of $P(O_3)_{\text{net}}$ is referred to as the measurement precision of the NPOPR detection system, which is different with the measurement accuracy of the NPOPR detection system described above."

I think this is certainly the case for the model, considering the VOC coverage (correctly) identified and uncertainties in e.g. knowledge of HONO (not measured directly), and I would ask the authors to consider carefully if the measured $P(O_3)$ is really good to 10% accuracy – and hence if quite such an extensive set of analysis is warranted. I'm conscious that lots of things will more-or-less co-vary diurnally within the measurement uncertainty (concentrations, j, T, $O_3...$) – is it really possible to extract missing reactants at a few % accuracy from within the combined measurement and model uncertainties?

Thank you for your insightful comment. We have thoroughly discussed the measurement error (precision) and accuracy of the custom-made NPOPR detection system, as described above. The evaluated measurement uncertainty of the $P(O_3)_{net}$ during the observation period are shown in Fig. S13. We see that the measurement uncertainty decreased with increasing $P(O_3)_{net}$ values, which ranges from 0-23%.

"

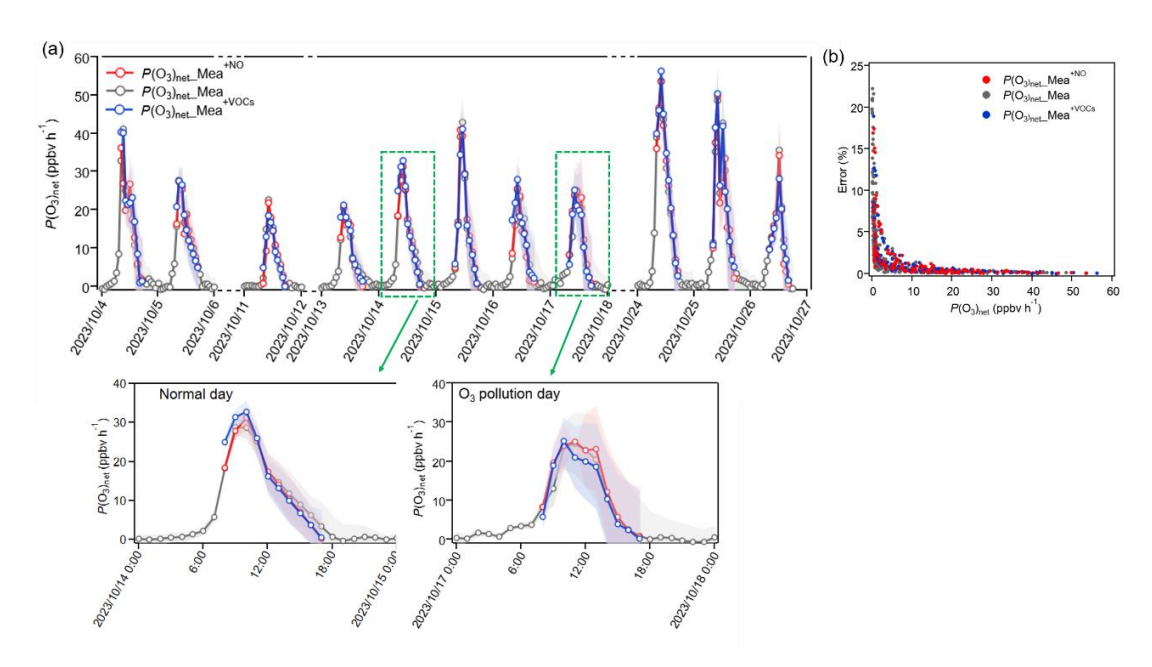


Figure S13: (a) Time series of measured $P(O_3)_{\text{net}}$ _Mea, $P(O_3)_{\text{net}}$ ^{+NO} and $P(O_3)_{\text{net}}$ ^{+VOCs} based on sensitivity experiments using the NPOPR detection system, with an enlarged view for an O_3 pollution day (October 26, 2023) and a normal (O_3 non-pollution) day (October 13, 2023). The shaded areas represent the errors of each measured term, calculated from the instrument measurement uncertainties given in Hao et al. (2023). (b) Relative errors of measured $P(O_3)_{\text{net}}$ _Mea, $P(O_3)_{\text{net}}$ ^{+NO}, and $P(O_3)_{\text{net}}$ ^{+VOCs} as a function of their measured values, ..."

More details concerning the measurement uncertainty are added in lines 503-506 in the modified manuscript: "The time series of measured $P(O_3)_{net}$ Mea, $P(O_3)_{net}$ had $P(O_3)_{net}$ based on sensitivity experiments using the NPOPR detection system are shown in Fig. S13. We see the measurement uncertainty decreased with increasing $P(O_3)_{net}$ values: it reaches approximately 23% when $P(O_3)_{net}$ is around 0 ppbv h⁻¹, but falls below 3% when $P(O_3)_{net}$ is around 50 ppbv h⁻¹."

Fig. S13b shows that the higher measurement uncertainty usually appears when the $P(O_3)_{\text{net}}$ is relatively low (e.g., in the early morning, evening, or late afternoon), whereas the relatively large $P(O_3)_{\text{net}}$ missing occur mainly around noon. The different diurnal patterns of measurement uncertainty (caused by concentrations, j, T, $O_3...$) and the modelling bias responsible for the $P(O_3)_{\text{net}}$ missing indicate that the two do not co-vary on a diurnal basis. The $P(O_3)_{\text{net}}$ missing may be small when averaged over daytime; however, it can reach \sim 33% around noon. This value is much higher than the measurement uncertainty

at that time (< 3%), making it possible to quantify the $P(O_3)_{net}$ missing in the model within a few percent. We added this discussion in lines 406-408 of the modified manuscript:

"Accurate quantification of $P(O_3)_{net}$ missing is possible here because the diurnal patterns of measurement uncertainty and the modelling bias responsible for the $P(O_3)_{net}$ missing do not covary; consequently, measurement uncertainty is much smaller than modelling bias for most of the daytime, especially around noon."

Showing more raw data – maybe 2-3 individual days plotted in detail so the measured and modelled data can be made out – would help the reader understand the sensitivities of the various metrics, alongside the "integrated" plots of sensitivities. This might help focus the manuscript also, as the story would be clearer with fewer analyses (and fewer SI figures) which would then also give confidence that the degree of analysis is appropriate and the data not over-interpreted.

Thank you for your suggestion. We have enlarged view for an O_3 pollution day (October 26, 2023) and a normal (O_3 non-pollution) day (October 14, 2023) in Figs. 3, 5, and S13 (as shown below).

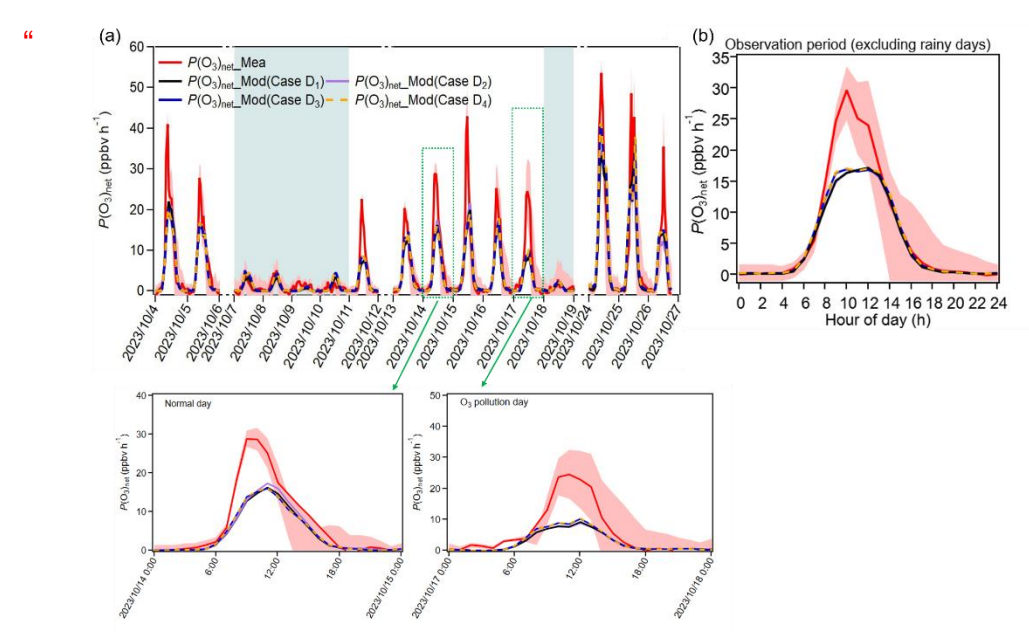


Figure 3: The time series and diurnal variations of $P(O_3)_{net}$ Mea and $P(O_3)_{net}$ Mod (Case D_1 - D_4) during the observation period, with an enlarged view for an O_3 pollution day

(October 26, 2023) and a normal (O₃ non-pollution) day (October 14, 2023); The shaded areas in (a) represent rainy days.

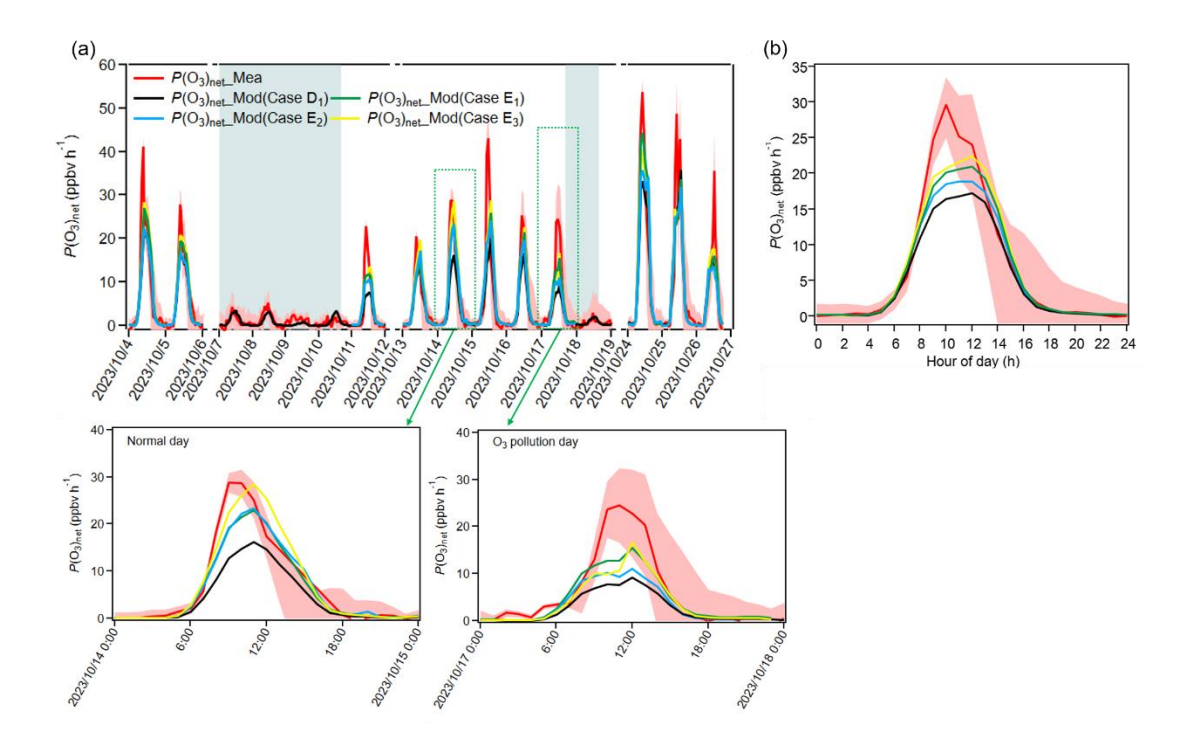


Figure 5: (a) Time series and (b) diurnal variations of $P(O_3)_{net}$ Mea and $P(O_3)_{net}$ Mod (Case D_1 – E_3) during the observation period, with an enlarged view for an O_3 pollution day (October 26, 2023) and a normal (O_3 non-pollution) day (October 14, 2023); (b) Diurnal variations excluding rainy days. The shaded areas in (a) represent rainy days.

From Fig. 3a, we see the modelled results on individual days varies, which make the $P(O_3)_{\text{net}}$ missing different with the overall diurnal variation (shown in Fig. 3b). For example, $P(O_3)_{\text{net}}$ Mod of Case D2 increased more on 17 October 2023 than that on October 14 2023, while $P(O_3)_{\text{net}}$ Mod of Cases D3-D4 increased more on October 17 2023 than that on October 14 2023. These results indicated that the overall increasing or decreasing trends can't represent all individual days during the observation period. On the other hand, the constraining of more OVOCs only corrects the outcome, not the related reaction processes. For example, the RO₂ radicals, which are the main intermediates that drive the oxidation chain during photochemical O₃ formation, may vary day-to-day. We added the related description for Fig. 3 in lines 339-341 of the modified manuscript:

"Furthermore, the enlarged days in Fig. 2 reveal day-to-day variations in $P(O_3)_{net}$ Mod across the different cases, underscoring that the overall diurnal pattern described above does not resolve this variability."

We added the related description for Fig. 5 in lines 492-494 of the modified manuscript:

"However, we observe a slight difference in the diurnal trends of $P(O_3)_{net}$ across different days (enlarged view in Fig. 5); this depicts the overall pattern for the observation period described above does not capture day-to-day variability."

We detected an error when check the $P(O_3)_{net}$ _Mod data from Case D_2 and Case D1, the overall daytime $P(O_3)_{net}$ _Mod from Case D2 showed a slightly decreasing trend (0.5%) compared to $P(O_3)_{net}$ _Mod from Case D1, therefore, we have changed the sentence "However, the daytime average value of $P(O_3)_{net}$ _Mod from Case D_2 increased by only 0.5% compared to Case D_1 , this indicates that the dominant OVOCs species that causes $P(O_3)_{net}$ _Missing may vary between Heshan and Dongguan." to "However, the daytime mean $P(O_3)_{net}$ _Mod in Case D_2 decreased by 0.5% compared with Case D_1 , indicating that the dominant OVOC species responsible for $P(O_3)_{net}$ _Missing may differ between Heshan and Dongguan." in lines 390-391 of the modified manuscript.

I recognise the method is published in the Hao et al (2023) paper, but would encourage the authors to include more discussion of measurement uncertainties here, and at the least a detailed justification of the statement "...measurement uncertainties around 10%" (L79). this should include, separately, accuracy, precision, and selectivity/bias – the impact of wall artefacts on the measured P(O3), which may vary with conditions (j, RH, VOC/NOx levels), and would best appear around L120.

Thank you for your suggestion. The relevant discussion and data analysis of measurement uncertainty of the custom-made NPOPR detection system are provided above. In summary, our measurement error is calculated in real time based on the light intensity and the Ox concentrations of the ambient air. As mentioned above, the related experiments and data analysis are shown in the Supplementary Materials S1. The related discussion has been added in lines 127-137 of the modified manuscript:

"The mean residence time in the reaction chamber is 0.15 h at the air flow rate of 2.1 L min⁻¹, and the limit of detection (LOD) of the NPOPR detection system is 0.86 ppbv h⁻¹ at the sampling air flow rate of 2.1 L min⁻¹, which is obtained as three times the measurement error of $P(O_3)_{net}$ (Hao et al., 2023). The measurement error of $P(O_3)_{net}$ is determined by the uncertainty in the Ox mixing ratio estimated for both the reaction and reference chambers. This uncertainty combines (i) the measurement uncertainty of the CAPS-NO₂ monitor used to derive Ox and (ii) the error induced by light-enhanced O₃ loss inside the chambers. Taken together, these contributions define the measurement precision of the NPOPR detection system. In addition, the measurement accuracy of the NPOPR detection system is 13.9 %, corresponding to the maximum systematic error arising from photochemical O₃ production in the reference chamber (Hao et al., 2023; Zhou et al., 2024b); details are given in Sect. S1 in the supplementary materials."

Furthermore, we checked the measurement uncertainties of different O₃ production sensors worldwide and confirmed that the uncertainties ranged from 10-30%. Therefore, we have changed the sentence to "Through practical applications in field observations, scholars generally agree that these detection systems offer rapid stability and high precision, with measurement uncertainties ranged from 10-30 %." in line 84 of the modified manuscript.

Corrections / Comments

L47 and following – it would be useful to distinguish between NO titration of O3 – ie NOx/O3 PSS shifts – and net production of Ox (which is what we really mean by ozone production). Several points in the text later (eg L134) there is reference to titration reducing ozone production – I'd argue that this is PSS shift, not a change in the ozone production chemistry, and a different terminology might help.

We apologize for the ambiguous description. We have changed the sentence to: "IR is defined as the change in $P(O_3)_{net}$ per unit change in precursor concentration ($\Delta S(X)$): a negative IR value indicates that reducing the precursor concentration increases O_3 production (e.g., decrease NOx would increase O_3 through OH mediate effect), ..." in line 156 of the modified manuscript.

Furthermore, we changed "This midday transition to NO_X-limited conditions is chemically reasonable, where intensified NO₂ photolysis boosts O_X production while

concurrently diminished NO titration and declining VOCs emissions collectively favor NO_X-sensitive chemistry during peak sunlight hours (Wang et al., 2023)." to "This midday transition to NO_X-limited conditions is chemically reasonable, where intensified NO₂ photolysis boosts O_X production while persistent photochemistry consumption without replenishment (Wang et al., 2023)." In lines 512-513 of the modified manuscript to make the description clearer.

L77 please acknowledge / include the pioneering work of Brune and colleagues (Cazorla et al., 2012) as the first "modern" MOPS system developers (I realise this is referenced later).

Thank you for your reminder. We have added the pioneering work of Brune and Cazorla as references (Cazorla and Brune, 2009; Cazorla et al., 2012) in line 81 of the modified manuscript:

"To date, several $P(O_3)_{net}$ detection systems based on the dual-reaction chamber technique have been developed, referred to as measurement of O_3 production sensor (MOPS), O_3 production rate measurement system (O3PR), O_3 production rates instrument (OPRs), net photochemical O_3 production rate detection system (NPOPR), Mea-OPR, or O_3 production rate-cavity ringdown spectroscopy system (OPR-CRDS) (Baier et al., 2015; Cazorla and Brune, 2009; Cazorla et al., 2012; Sadanaga et al., 2017; Sklaveniti et al., 2018; Hao et al., 2023; Wang et al., 2024c; Tong et al., 2025)."

L79 Measurement uncertainties – I do not think 10% is realistic – see general comments above

We apologize that we made a mistake here. As mentioned above, we checked the measurement uncertainties of different O₃ production sensors worldwide and confirmed that the uncertainties ranged from 10-30%. Therefore, we have changed the sentence to "Through practical applications in field observations, scholars generally agree that these detection systems offer rapid stability and high precision, with measurement uncertainties ranged from 10-30 %." in the modified manuscript.

L100 is there much emission / chemical heterogeneity around the site? e.g. on the timescale of NOx PSS (1 min+) or HONO PSS (10-15min+)?

Thank you for your thoughtful consideration. The observation site, the Guangdong Atmospheric Supersite of China, is located in a farmland conservation zone and forested region at the suburban area of Heshan City. There are no major local industrial emission sources and the motorcycles dominate urban transport in Heshan City. However, the supersite experiences minimal spatial heterogeneity in either primary emissions or chemical composition as it is located on a small mountain approximately 3 km from the nearest area with heavy traffic emissions. With a mean wind speed is 2.8 m s⁻¹ during the observation period, the air mass originating from the traffic corridor requires ~ 17 min to reach the supersite; consequently, rapid dilution and initial photochemical processing of exhaust plumes occur before they reach the supersite.

We changed the sentence "The supersite is situated in the downwind area of Guangzhou and Foshan and is characterized by active secondary reactions. It lies at the intersection of forest-agricultural and urban systems, representing a typical rural station. The surrounding area primarily consists of farmland conservation zones and forested areas, with no significant industrial emissions. It is suitable for comprehensive monitoring and research on regional atmospheric complex pollution in the PRD (Mazaheri et al., 2019)." to "The supersite is situated in the downwind area of Guangzhou, Foshan, and Dongguan, a region characterized by active secondary reactions and serving as a receptor for pollution transported from the industrial and urban centers (Luo et al., 2025; Huang et al., 2020). The surrounding area is primarily composed of farmland conservation zones and forested regions, with no major industrial sources. The supersite sits on a small mountain ~ 3 km from the nearest area heavy traffic corridor; at the observed mean wind speed of 2.8 m s⁻¹, the air mass from the corridor takes ~ 17 min to arrive. This separation limits spatial heterogeneity in both emissions and chemical composition, making the site well-suited for comprehensive monitoring and research on complex regional air pollution in the PRD (Mazaheri et al., 2019)." in lines 104-111 of the modified manuscript.

L131 Explain how the VOC addition amounts were determined/apportioned between the two species

According to the previous study, the selection of the VOCs indicator for the O₃ formation sensitivity measurement can be determined using the VOCs measured previous to the O₃ formation sensitivity (OFS) measurements (Carter

et al., 1995; Wu et al., 2022). We first calculated the total VOCs reactivity using the daytime VOCs measured from 20 September to 3 October and from 4-11 October 2023 at the observation site. For the OFS measurement from 4-11 October, we used the total VOCs reactivity measured from 20 September to 3 October 2023, VOCs indicators included isopentane as the representative alkane, ethylene and isoprene as the representative alkenes, and toluene as the representative aromatic hydrocarbon. From 13-26 October, we used the averaged daytime total VOCs reactivity measured from 4 to 11 October 2023, VOCs indicators included Ethylene was used as the representative nonmethane hydrocarbon (NMHC) indicator and formaldehyde as the representative oxygenated volatile organic compound (OVOC) indicator. The related description is added in lines 143-151 of the modified manuscript:

"Following Carter et al. (1995) and Wu et al. (2022), we select VOCs surrogates for the OFS measurement on the basis of ambient measurements previous to the measurements. From 4–11 October, the tracer mixture was formulated from the average daytime total VOC reactivity measured during 20 September–3 October 2023, and isopentane served as the alkane surrogate, ethylene and isoprene as the alkene surrogates, and toluene as the aromatic surrogate. For 13–26 October 2023, we used the average daytime total VOC reactivity obtained during 4–11 October 2023; ethylene represented non-methane hydrocarbons (NMHCs) and formaldehyde represented oxygenated VOCs (OVOCs). Each surrogate was mixed in proportion to its category's share of the ambient reactivity, and the effective precursor strength (NO or VOCs) should increase by 20 % relative to the original ambient level."

L202 E10 – I do not follow how the net P(O3) is equal to P(O3) multiplied by the change in P(O3) divided by the (natural log of) change in X.

We apologize for the error in the equation expression. The description has been revised in lines 223-227 of the modified manuscript:

"We calculated the modelled OFS using the absolute $P(O_3)_{net}$ sensitivity, adapted from the logarithmic derivative approach of Sakamoto et al. (2019). It is defined as the change in $P(O_3)_{net}$ with respect to the natural logarithm of O_3 precursor concentrations. This method facilitates the quantitative assessment of how reductions in O_3 precursors contribute to the overall reduction of $P(O_3)_{net}$ over a period or within a region. The formula is as follows:

Absolute
$$P(O_3)_{\text{net}} = \frac{dP(O_3)_{\text{net}}}{d \ln[X]}$$
 (10)

L234 not sure "stronger" photochemical reactions is right word – do you mean higher photolysis rates? An alternative explanation for the (slightly) lower concs might be greater solar heating/higher BLH/more dilution on the hotter/sunnier/higher P(O3) days – evidence in the BLH data?

Thank you for your suggestion. Yes, we mean higher photolysis rates occur on O_3 pollution days (see Fig. S4a). We further checked the planetary boundary-layer height (PBLH) on both O_3 pollution days and normal days. We found that in the morning the PBLH was higher on O_3 pollution days, whereas in the afternoon it became lower than on normal days (see Fig. S4k). During the period of strongest sunlight (11:00-14:00), the PBLH on O_3 pollution days and normal days does not appear statistically different (*t-test*, p=0.45). Therefore, the lower concentrations of TVOC and NO_X on O_3 pollution days compared with normal are not likely due to changes in PBLH change or increased dilution.

Accordingly, we have changed the description from "This suggests that stronger photochemical reactions occur on O₃ pollution days, leading to lower daytime concentrations of precursors compared to normal days." to "As the PBLH on O₃ pollution days and normal days does not differ statistically during the period of strongest solar radiation (11:00-14:00, *t*-test, *p*=0.45, see Fig. S4k), the lower daytime concentrations/mixing ratios of O₃ precursors on O₃ pollution days than on normal days may be due to higher photolysis rates on O₃ pollution days (see Fig. S4a)." in lines 257-259 in the modified manuscript.

L305 give the missing P(O3) as a % also – maybe 24 hour mean. Statistical test – I assume *P* level of 0.05 not 0.5?

Sorry for the confusion description. We have modified the sentence to make it clearer, as shown in lines 338-343 in the modified manuscript:

"On non-rainy days, the averaged daytime $P(O_3)_{net}$ Missing reached 4.5±7.6 ppbv h⁻¹, accounting for 31% of the total measured $P(O_3)_{net}$. The averaged daytime $P(O_3)_{net}$ Missing values on O_3 pollution days were statistically higher than those on normal days (*t-test*, p<0.05), suggesting that while the supplementary mechanisms explored in the model may contribute to

some extent, they are unlikely to be the dominant cause of the $P(O_3)_{net}$ Missing."

L325+: Is there really sensitivity in the correlations to identify particular causes?

Thank you for your question. The correlation analysis is only a preliminary examination of the factors that may be related to the $P(O_3)_{\text{net}}$ _Missing in the model, aimed at guiding further investigation; it therefore does not allow us to identify specific causes. We have softened the wording in the sentences in lines 367 to 374in the modified manuscript:

"To explore the possible drivers of $P(O_3)_{net}$ Missing, we correlated it with TVOC, NO_X, J_{O1D} , T, and O_X separately for O₃ pollution days and normal days (Fig. S11). On O₃ pollution days, $P(O_3)_{net}$ Missing exhibited a moderate positive correlation with VOCs ($r^2 = 0.4$, R = 0.2, t = 2.9) and NO_X ($r^2 = 0.5$, R = 0.2, t = 3.8), confirming that the $P(O_3)_{net}$ Missing is larger at higher precursor concentrations/mixing ratios (both t > critical 2.0, p < 0.05), consistent with earlier box-model studies (Whalley et al., 2021; Ren et al., 2013; Zhou et al., 2024a). A moderate positive correlation is also found with J_{O1D} on both O₃ pollution days and normal days, with r^2 values of 0.5 and 0.4, respectively. On normal days all correlations collapse ($r^2 < 0.2$, p > 0.1), implying that the model deficit is not tied to the measured precursors under low-NO_x conditions and may instead related to the missing mechanisms for unmeasured photolabile VOCs."

L345 is it valuable to include all of D1-D4 – cut straight to the final case, D4?

By setting different simulated scenarios from Cases D1–D4, we primarily wanted to check quantitively whether the additional mechanisms and the measured OVOCs have a significant influence on $P(O_3)_{net}$ _Missing. The configurations of each scenario are as follows: Case A considers only the simplified chemical reaction mechanism from MCM v3.3.1; Case B incorporates the HO₂ uptake by ambient aerosols mechanism based on Case A; Case C further includes the dry deposition processes of key species on top of Case B; Case D1 extends Case C by adding the N₂O₅ uptake mechanism and CI-related heterogeneous reaction mechanisms. Case D2 includes the measured OVOCs based on Case D1— namely, acetaldehyde, acrolein, acetone, and butanone—which were considered qualitatively as potential contributors to $P(O_3)_{net}$ _Missing in Dongguan in our previous study (Zhou et al., 2024); Case D3 constrained all measured OVOC species in Heshan based on Case D2;

Case D4 constrained chlorine-containing VOCs (i.e., all measured VOC species listed in Table S8 that could be input into the OBM model). Detailed simulation parameter settings are provided in the main text and the Supplementary Materials (Table S3). We believe that this step-by-step simulation process is necessary for a better understanding of the different mechanisms and the impact of OVOCs on $P(O_3)_{net}$ _Missing.

Fig S13 – It is very hard to see the change in *P*O₃ from the added NO/added VOCs – suggest show a zoom in on a polluted/non-polluted day in addition so the data can be seen. The uncertainty ranges look very small on this figure?

Thank you for your suggestion. We have added a zoom in on a O_3 pollution day (October 26, 2023) and a normal (O_3 non-pollution) day (October 13, 2023) in Fig. S13 to make it clearer.

"

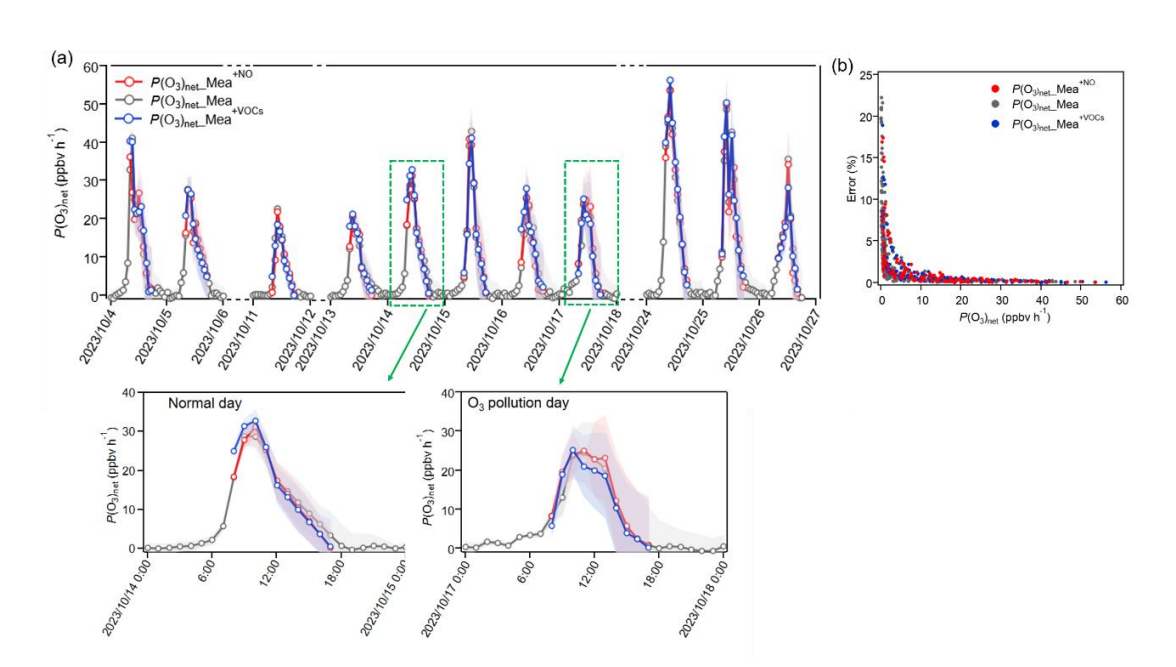


Figure S13: (a) Time series of measured $P(O_3)_{\text{net}}$ _Mea, $P(O_3)_{\text{net}}^{+NO}$ and $P(O_3)_{\text{net}}^{+VOCs}$ based on sensitivity experiments using the NPOPR detection system, with an enlarged view for an O_3 pollution day (October 26, 2023) and a normal (O₃ non-pollution) day (October 14, 2023). The shaded areas represent the errors of each measured term, calculated from the instrument measurement uncertainties given in Hao et al. (2023); (b) Relative errors of measured $P(O_3)_{\text{net}}$ _Mea, $P(O_3)_{\text{net}}^{+NO}$, and $P(O_3)_{\text{net}}^{+VOCs}$ as a function of their measured values; ...

The measurement uncertainties, shown as shaded areas in Fig. S13, are calculated as the measurement error described in Hao et al. (2023) and Zhou et al. (2024): when injecting ambient air into the NPOPR system, the error of $P(O_3)_{net}$ with a residence time of τ can be calculated using this equation:

$$P(O_3)_{\text{net_error}} = \sqrt{(O_{X\gamma})_{\text{rea_error}}^2 + ((9.72 \times [(O_X]_{\text{rea_measured}})_{\text{rea_std}}^{-1.0024})_{\text{rea_std}}^2 + ((9.72 \times [(O_X]_{\text{ref_measured}})_{\text{ref_std}}^{-1.0024})_{\text{ref_error}}^2 + ((9.72 \times [(O_X]_{\text{ref_measured}})_{\text{ref_std}}^{-1.0024})_{\text{ref_std}}^2 + ((9.72 \times [(O_X]_{\text{ref_measured}})_{\text{ref_std}}^2 + ((9.72 \times [(O_X]_{\text{ref_std}})_{\text{ref_std}}^2 + ((9.72 \times$$

 $(O_{X\gamma})_{rea_error}$ and $(O_{X\gamma})_{ref_error}$ represent the measurement error due to light-enhanced loss of O₃ in the reaction and reference chambers, respectively, and $(9.72\times[O_X]_{measured}^{-1.0024})_{rea_std}$ and $(9.72\times[O_X]_{measured}^{-1.0024})_{ref_std}$ represent the standard deviation of O_X in the reaction and reference chambers, respectively, caused by the CAPS NO₂ monitor with an integration time period of 100 s. Combined with the associated residence time $\langle \tau \rangle$ under different flow rates, i.e., $\langle \tau \rangle$ was 0.063 h at a flow rate of 5 L min⁻¹. Therefore, the instrument measurement error is determined by the measurement error of O_X in the reaction and reference chambers, which may also be influence by the lightenhanced loss of O_X in the reaction and reference chambers under ambient conditions when the light intensity (especially J(O1D)) and O₃ mixing ratios are high. The related description is added now in the Supplementary Materials S1.

To check the relative error of $P(O_3)_{net}$ _Mea, $P(O_3)_{net}$ ^{NO} and $P(O_3)_{net}$ ^{VOCs}, we plotted the measurement error as a function of their measured values (see Fig. S13b). We find that the uncertainty decreased with increasing data values: it reaches approximately 23% when $P(O_3)_{net}$ is around 0 ppbv h⁻¹, but falls below 3% when $P(O_3)_{net}$ is around 50 ppbv h⁻¹.

We have now added such kind of description in lines 503-506 in the modified manuscript: "The time series of measured $P(O_3)_{\text{net}}$ _Mea, $P(O_3)_{\text{net}}$ _{NO}^{+NO} and $P(O_3)_{\text{net}}$ _{VOCs}^{+VOCs} based on sensitivity experiments using the NPOPR detection system are shown in Fig. S13. We see the measurement uncertainty decreased with increasing $P(O_3)_{\text{net}}$ values: it reaches approximately 23% when $P(O_3)_{\text{net}}$ is around 0 ppbv h⁻¹, but falls below 3% when $P(O_3)_{\text{net}}$ is around 50 ppbv h⁻¹."

L440ish: Ozone regime – there is only one data point in the afternoon showing a VOC limited regime (14:00). Is there really a shift from VOC to NOx to VOC to NOx limited through the day – can the data really show this? I am conscious that there are not many days going into these averages. How is "transition regime" defined for the measurements? The explanation (L442): P(O3) measurement is not affected by NOx/O3 titration (or PSS) – rather it measures change in the net Ox production.

Yes, we obtained only one data point showing a VOC-limited regime in the afternoon from the direct measurement. However, this diurnal profile shown in Fig. S14 is compiled from all days on which O₃ formation sensitivity was directly measured; it represents the overall trend during the observation period and does not reflect the day-to-day variation. As described in the main text, in total 11 days were incorporated into this calculation during the observation period, which includes 4–5, 11, 13–17, and 24–26 October 2023. We added the related discussion in lines 507-509 of the modified manuscript:

"Fig. S14 shows the diurnal variation of the directly measured IR index compiled from all 11 days of OFS experiments, together with the absolute $P(O_3)_{net}$ sensitivity to NO_X and VOCs calculated with the box model (Case D_1 , Eq. (10)). It therefore depicts the overall trend across the observation period and does not reflect the day-to-day variability."

Here, we define the transition regime as the region over which the IR shows a simultaneous increase or decrease upon addition of both VOCs and NO. We added it in lines 161-162 in Sect. 2.1. "We define the transition regime as the region over which the IR shows a simultaneous increase or decrease upon addition of both VOCs and NO."

Since we are measuring $P(O_3)_{net}$ in our NPOPR detection system, the measurement result is not affected by NOx/O₃ titration (or PSS), we have modified the sentence "This midday transition to NO_X-limited conditions is chemically reasonable, where intensified NO₂ photolysis boosts O_X production while concurrently diminished NO titration and declining VOCs emissions collectively favor NO_X-sensitive chemistry during peak sunlight hours (Wang et al., 2023)." to "This midday transition to NO_X-limited conditions is chemically reasonable, where intensified NO₂ photolysis boosts O_X

production while persistent photochemistry consumption without replenishment (Wang et al., 2023)." in lines 511-513 of the modified manuscript.

Fig 6 – please show the mean diurnals for PO3 (from the measurements) for the three regimes identified. Not sure that the rapid changes in emissions can be the explanation – the model is constrained to the observed concentrations, so it has this "built in".

Thank you for your suggestion. We have now conducted the mean diurnal cycles of $P(O_3)_{net}$ for the three regimes identified from the direct measurements. The O_3 formation sensitivity (OFS) of each day was diagnosed from its daily-integrated measurements; the mean diurnal variation for all days within the same OFS category was calculated. In total, eight days were classified as transition regime (4-5, 11, 14-15, 24-26 October 2023), two as VOC-limited regime (13 and 16 October 2023), and one as NOx-limited regime (17 October 2023). The resulting diurnal profiles are shown in Fig. S13c-d. Between 08:00 and 12:00 the mean diurnal profiles reveal a gradual shift from VOC-limited toward NO_x-limited conditions within the VOC-limited category, and a similar progression from transition to NO_x-limited within the transition category. We added the related description in lines 536-539 of the modified manuscript:

"To illustrate that the diurnal shift in OFS depicted in Fig. 6 is not random noise but reflects the general rule, we grouped the 11 days of direct measurements by their initial O₃-formation regime, calculated their average diurnal variations, and thus reproduced the "morning-transition" phenomenon in Fig. S13c–d."

And added the mean diurnal variation of $P(O_3)_{net}$ for the three regimes in Fig. S13c-d:

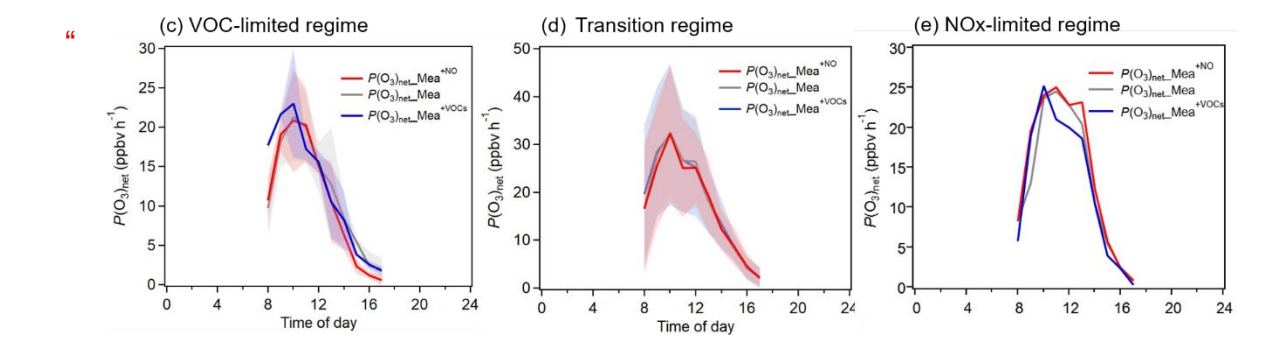


Figure S13: ... (c-e) Mean diurnal profiles of the three O₃ formation regimes identified: eight days classified as transition regime (4-5, 11, 14-15, 24-26 October 2023, two as VOC-limited regime (13 and 16 October 2023), and one as NOx-limited regime (17 October 2023)."

We agree with the reviewer that the mean diurnal variations in O₃ formation sensitivity (OFS) are not influenced by rapid emission changes. As mentioned above, the site is situated on a small mountain ~3 km from the nearest heavy-traffic corridor; at the observed mean wind speed of 2.8 m s⁻¹, an air mass from the corridor takes ~17 min to arrive. This separation reduces spatial heterogeneity in both emissions and chemical composition at the observation site (see Sect. 2.1 of the revised manuscript).

A greater challenge in this regard may be the P(O3) measurements which average over an hour effectively?

We designed experiments to determine the OFS from direct measurements conducted daily from 8:00-18:00. Each measurement cycle lasted 1 hour: the first 20 min consisted of NO addition (denoted $P(O_3)_{net}$ _Mea^{+NO}), the next 20 min of ambient baseline measurement ($P(O_3)_{net}$ _Mea), and the final 20 min of VOCs addition ($P(O_3)_{net}$ _Mea^{+VOCs}). Therefore, we first interpolated $P(O_3)_{net}$ _Mea^{+NO}, $P(O_3)_{net}$ _Mea, and $P(O_3)_{net}$ _Mea^{+VOCs} to 4-min resolution and then averaged these values over 1 h to eliminate the influence of the data fluctuation. However, the 1-hour averaging may smooth out transient responses of the measured $P(O_3)_{net}$. The related description is now added in lines 151-153 in the modified manuscript:

"For data treatment, we first interpolated $P(O_3)_{net}$ _Mea^{+NO}, $P(O_3)_{net}$ _Mea, and $P(O_3)_{net}$ _Mea^{+VOCs} to 4-min resolution and then averaged them over 1 h to suppress data fluctuations. We caution that this 1-hour averaging may smooth out transient responses in the measured $P(O_3)_{net}$."

Isnt it more that you have already shown that the model (not unexpectedly) has bias from missing VOCs and this is reflected in these analyses also?

Yes, we have shown that the bias in the model may be attributed to missing VOCs, as reflected by the comparison of OFS results obtained from direct

measurements and from modeling cases D1 and E1–E3 during the rising, stable, and declining phases of $P(O_3)_{net}$ (as described in Sect. 4). Briefly, in modeling cases where $P(O_3)_{net}$ Missing was reduced (Cases E1–E3), the simulated OFS occasionally shifted toward NOx-limited conditions during certain periods. This contradictory phenomenon may be related to the model's incomplete representation of the chemical mechanisms of unknown highly reactive VOCs (e.g., aldehydes and ketones), which is consistent with previous studies suggesting that diagnostic methods based on box models tend to overestimate VOC sensitivity due to the neglect of unidentified VOCs in anthropogenic emissions or their secondary products (Xu et al., 2022; Lu et al., 2010).

Therefore, we deleted the sentence "This low consistency may be related to rapid changes in precursor concentrations in the morning: the concentrations of VOCs and NO_X concentrations change quickly during this period, particularly due to traffic emissions and industrial activities. These rapid variations make it challenging for the model to accurately capture the instantaneous reaction dynamics (Cao et al., 2021).", and added "These results demonstrate that the bias between measured and modeled OFS arises chiefly from missing VOCs or shortcomings in the model's chemical mechanism." in lines 551-552 to explain the reason for the inconsistency between OFS derived from the direct measurement and the model simulation methods.

L489/Fig S15 – what are cases E1-E3? Not mentioned previously and I cannot find a definition / description of these. I cannot follow L490-L505 as these cases/ scenarios are not defined

Sorry for the unclear description. In Case E1, the overall TVOC concentration was increased to compensate for k_{OH} _Missing without distinguishing VOCs categories. In Case E2, ethylene and formaldehyde were increased to compensate for k_{OH} _Missing. In Case E3, only formaldehyde concentration was expanded to compensate for k_{OH} _Missing. The detailed settings of each simulation case are listed in Table S3, and the explanations concerning Cases E1-E3 are listed in lines 476-484 in the modified manuscript:

"In Case E_1 , where the overall TVOC concentration was increased to compensate for $k_{\rm OH}$ _Missing without distinguishing VOCs categories, the compensation effect was limited due to the dilution effect of low-reactivity VOCs, resulting in a reduction of the daytime average $P(O_3)_{\rm net}$ _Missing proportion from 26.3 % (calculated as $P(O_3)_{\rm net}$ _Missing/ $P(O_3)_{\rm net}$ _Mea) to 10.3 %. In Case E_2 , where the concentrations of ethylene and formaldehyde were expanded to compensate for $k_{\rm OH}$ _Missing, the daytime average $P(O_3)_{\rm net}$ _Missing proportion reduced from 26.3 % to 17.2 %. This proportion is higher than that obtained from Case E1, which may be due to the relatively low reactivity of ethylene limited the overall compensation effect. In contrast, Case E_3 compensated for $k_{\rm OH}$ _Missing solely by expanding the formaldehyde concentration. More details concerning the cases settings are shown in Table S3."

Conclusions – is there a comment to make on the impact of different chemical mechanisms (eg L65+) on the model/measurement agreement?

We have investigated the influence of some missing mechanisms in MCM v3.3.1, such as HO₂ uptake by ambient aerosols, dry deposition, N₂O₅ uptake, and ClNO₂ photolysis (Case D₁), to the modelling results. However, some other reaction mechanisms, such as the RO₂ isomerization (Crounse et al., 2012), autoxidation (Wang et al., 2017), and the accretion reactions (Berndt et al., 2018) can also effect modelled $P(O_3)_{net}$, but these processes have not been investigated in this study. Therefore, we have added a comment on the impact of different chemical mechanism as follows in lines 418-421 of the modified manuscript:

"Previous studies have shown that the RO_2 isomerization (Crounse et al., 2012), autoxidation (Wang et al., 2017), and the accretion reactions (Berndt et al., 2018) can also effect modelled $P(O_3)_{net}$, but these processes have not been investigated here."

And lines 584-588 of the modified manuscript:

"These results also demonstrate that incorporating the aforementioned missing mechanisms and measured VOC species cannot fully eliminate simulation bias. Other processes, i.e., the RO₂, autoxidation, and the accretion reactions can also affect modelled $P(O_3)_{net}$, but they have not been examined here. The negative correlation of $P(O_3)_{net}$ Missing with the air mass aging indicates that the $P(O_3)_{net}$ missing is not likely caused by unaccounted secondary production."

Conclusions – do you wish to add an overall comment vs the NOx- vs VOC-control on O₃ observed at the site, and implications for policy vs reducing ozone

formation rates? this might usefully also remind the reader of the distinction between the in-situ formation rate (focus here) and the total level experienced (integration of local formation and upwind chemistry / advection).

Yes, we have now added an overarching statement in lines 609-616 of the modified manuscript:

"In conclusion, we quantitatively assessed the $P(O_3)_{net}$ simulation deficits and their impact on OFS diagnosis by comparing the measured and modelled $P(O_3)_{net}$, and found that the unmeasured VOCs —rather than the secondary atmospheric formation —are the primary causative factor of $P(O_3)_{net}$ Missing. Furthermore, both direct measurements and model results reveal a diurnal OFS shift dominated by the morning regime; transition and VOC-limited conditions prevailed, so prioritizing VOCs while co-controlling NO_X is the most effective approach to O_3 pollution control in PRD region. Our results also demonstrate that the persistent model biases risk under-estimating the local photochemical formation contribution to O_3 pollution, thereby has weakening its perceived impact relative to physical transportation. Future studies should expanded VOCs measurements and combine direct $P(O_3)_{net}$ observations with regional transport model to separate local production from up-wind advection."

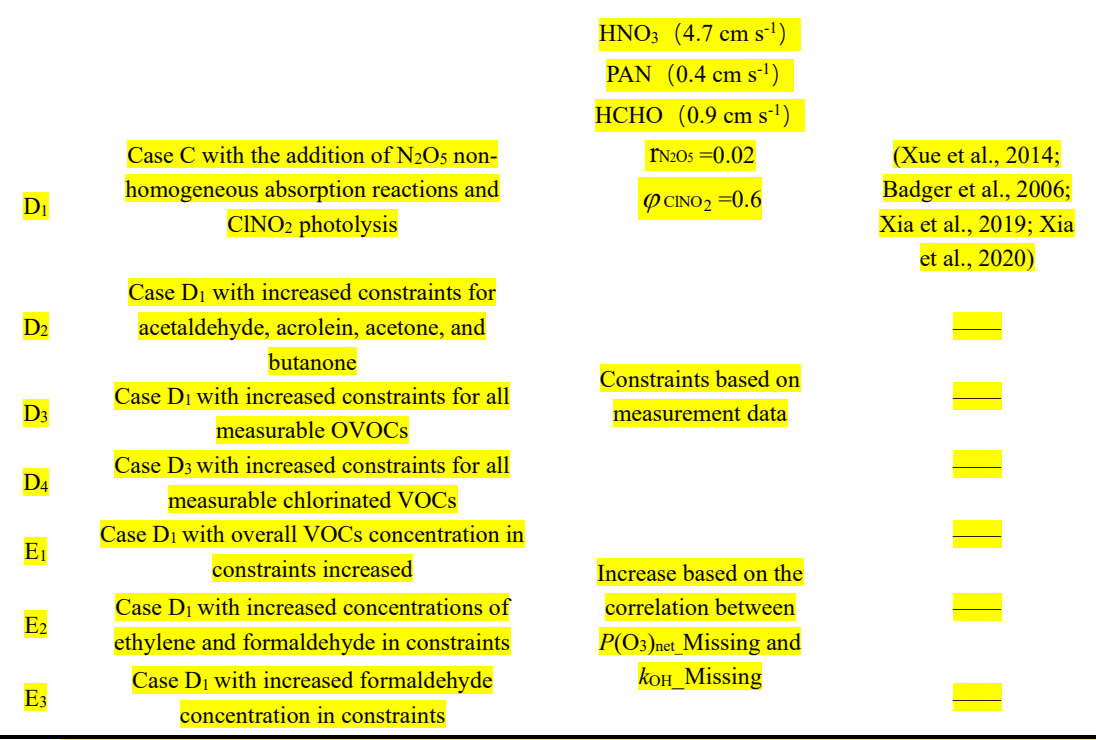
Model Approach Clarifications

-A summary table of the different scenarios, A-E, would be very helpful – I think this is referred to but I cannot find in the SI?

There is a detailed description of different modelling scenarios from A-E, as shown in Table S3 in the SI:

Table S3. Description of different modelling scenarios and the parameter settings

Case	Description	Parameter settings	references
A	Ambient gases (NO, NO2, SO2, CO, O3),	O_3 (0.27 cm s ⁻¹)	(Xue et al., 2014)
	HONO, 44 VOCs, meteorological		
	parameters (T, RH, P, BLH), photolysis		
	rates, and O ₃ dry deposition		
В	Case A with the addition of HO ₂ uptake	$r_{\rm H2O} = 0.19$	(Zhu et al., 2020;
			Zhou et al., 2021)
C	Case Bwith the addition of trace gases	$NO_2 (0.6 \text{ cm s}^{-1})$	(Zhang et al., 2003;
	(NO ₂ , SO ₂ , H ₂ O ₂ , HNO ₃ , PAN, HCHO) dry	$SO_2 (0.8 \text{ cm s}^{-1})$	Xue et al., 2014)
	<u>deposition</u>	H_2O_2 (1.2 cm s ⁻¹)	



Notes: Parameter values for modelling scenarios from Case A to Case D₁ are set the same as those in Zhou et al. (2024a).

-Model observation constraint: It would be helpful to explain how the constraint to observations was implemented – we have model outputs on an hourly basis but how frequently where the constraints applied to the model and did concentrations evolve freely in between (shorter model integration timestep)? If the model species are not in balance a "saw tooth" effect can result in the simulated concs at the higher model time resolution between observation constraint points – was this the case and if so impacts on the P(O3) which is in effect averaged over this period?

Thank you for your insightful suggestion. In this study, the box model was constrained by on-site observations of VOCs, NO, CO, HONO, and meteorological parameters (i.e., photolysis rates, RH, *T*, and P), as described in Sect. 2.2. Constraints were applied every hour, with no free concentration evolution in between. We have added the relevant description in lines 181–182 of the revised manuscript.

"The constraints are applied to the model every 1 h, with no free concentration evolution in between."

From Figs.3, 5, and S13, we do not see the "saw tooth" effect. Unfortunately, the data obtained in this campaign were mostly in 1 hour time resolution, thus we cannot evaluate how the model behaves at sub-hourly resolution between constraint points. We regard this as a critical issue that could materially affect modelled $P(O_3)_{net}$ and will therefore be addressed explicitly in our next study.

-Approach to HONO – tucked away in the SI, the use of MARGA measurements of soluble nitrite for gas-phase HONO is mentioned. I appreciate that some approach was needed, but the sensitivity of the model results to this assumption is needed – eg what shift in P(O3) does a 20% change in HONO concs (or whatever is reasonable) result in. If this is a large shift – are the subsequent analysis all valid, i.e. can you be confident in pushing the model explorations so far? What is the time resolution of the MARGA data vs the observed temporal variation of e.g. NOx?

Thank you for the suggestion. According to Xu et al. (2019), a large number of two-channel WD/IC instruments represented by the Monitor for AeRosols and Gases in ambient Air (MARGA) instruments was widely used to obtain aerosol composition information, as well as acid trace gas levels, including HONO (Stieger et al., 2018). However, the application of HONO data was limited because of the measurement uncertainty. The measurement uncertainty of HONO database obtained by MARGA was evaluated by Xu et al. (2019) and Spindler et al. (2003). For this purpose, Xu et al. (2019) used a MARGA and more accurate equipment (LOPAP) to simultaneously measure the HONO concentration at the Station for Observing Regional Processes of the Earth System (SORPES) in the YRD of east China; Spindler et al. (2003) performed the laboratory and field experiments as well as direct kinetic laboratory studies to quantify an artefact by the aqueous phase formation of HONO from dissolved NO₂ and SO₂ at wetted denuder walls. In this study, we used the method proposed by Spindler et al. (2003) to check the measurement error of HONO by MARGA, and then checked its influence to the modelled P(O₃)_{net}. More details are added in the Supplementary Materials S2.

"However, previous studies have shown the HONO may be overestimated by MARGA due to aqueous phase formation of HONO from dissolved NO₂ and SO₂ at wetted denuder walls

(Stieger et al., 2018; Spindler et al. 2003). The measurement error of HONO by MARGA was evaluated by Xu et al. (2019) and Spindler et al. (2003). In this study, we used the method proposed by Spindler et al. (2003) to evaluate measurement uncertainty of HONO database obtained by MARGA, and then checked its influence to the modelled $P(O_3)_{net}$. The overall artefact formation measurement error of HONO by MARGA is expressed as a sum in Eq. (S5):

$$[HNO_2]_{art} = 0.056[NO_2] + (0.0032/ppb)[NO_2][SO_2]$$
 (S5)

where 0.0032 is the reciprocal value of the slope of the straight line between the HNO₂ concentration corrected for the HNO₂ content in purified air, the mean NO₂ artefact and the concentration product of NO₂ and SO₂. We further modelled $P(Ox)_{net}$ Case D₄ with the corrected HONO, and found that the corrected HONO could decrease the modelled $P(Ox)_{net}$ Case D₄ by 0-8%, as shown in Fig. S18. Therefore, we note that with the measurement error of HONO by MARGA, the modelling method may consistently underestimate the modelled $P(Ox)_{net}$ in all cases, and the $P(Ox)_{net}$ missing in our study should be regarded as the lower limit values.

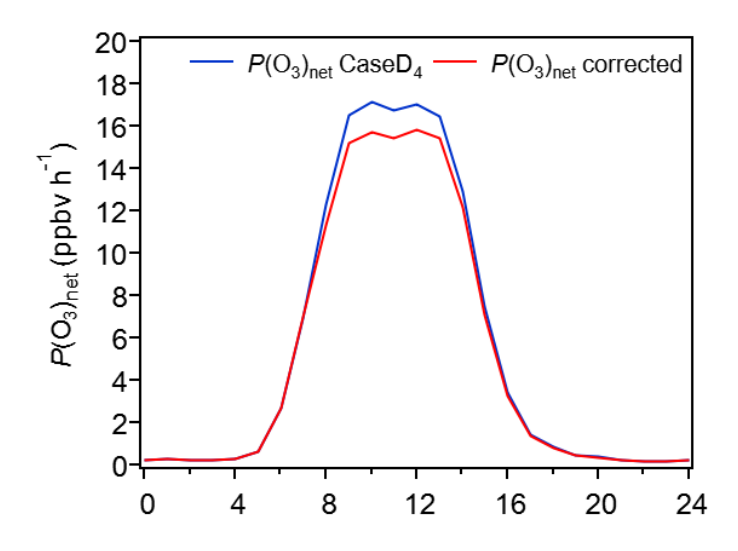


Figure S18: The modelled $P(Ox)_{net}$ Case D₄ and the with and without the HONO correction."

Accordingly, we added the related description in lines 334-336 of the modified manuscript:

"Due to the measurement error of HONO by MARGA in this study, the modelled $P(O_3)_{net}$ tends to be underestimated (as shown in SM: S2); thus, we define the $P(O_3)_{net}$ Missing obtained from all simulation cases as the upper-limit values."

And lines 574-576 of the modified manuscript:

"Systematic underestimation of modelled $P(O_3)_{net}$ ($P(O_3)_{net}$ Mod) was found when compared to the measured $P(O_3)_{net}$ ($P(O_3)_{net}$ Mea); this difference is defined as upper-limit $P(O_3)_{net}$ Missing due to the overestimation of HONO by MARGA in this study."

The nitrogen oxides analyzer (Fengyue Aorui-1014, China) provided NO_x data at a temporal resolution of 1 min, while the NO₂⁻ data from the MARGA were recorded at 1 h resolution. Therefore, all data were averaged to 1 h for model input, as stated in lines 163–165 of the main text.

"In addition to $P(O_3)_{net}$ and OFS, hourly data such as $PM_{2.5}$, O_3 , NO, NO_2 , SO_2 , carbon monoxide (CO), photolysis rates $(j_O^1D, j_{NO_2}, j_{H_2O_2}, j_{NO_3_M}, j_{NO_3_R}, j_{HONO}, j_{HCHO_M}, j_{HCHO_R})$, HONO, and VOCs concentrations were monitored (more details about the measurements are shown in Table S1)."

-Lots on the deposition velocities but how well do we know the boundary layer height BLH?

The planetary boundary layer height (PBLH) is the reanalysis data obtained from the website of the NOAA Air Resources Laboratory (https://ready.arl.noaa.gov/READYamet.php). The diurnal changes of PBLH on O₃ pollution days and normal days are added in Fig. S4 in the Supplementary Materials. We have provided an additional description on the source of the PBLH data in lines 167-169 in the revised manuscript:

"The PBLH data used in the model here was obtained from the web portal of the Real-time Environmental Applications and Display sYstem (READY) of the National Oceanic and Atmospheric Administration (NOAA) Air Resource Laboratory (https://ready.arl.noaa.gov/READYamet.php)."

L172 – is the HO₂ uptake process an irreversible loss (in the model)?

Yes, we used the data obtained from Zhou et al. (2020, 2023) measured from the ambient air and assumed it is an irreversible loss in the model.

L174 – is the N_2O_5 uptake an irreversible loss – if I follow some scenarios included recycling via $CINO_2$ – not quite clear how the condensed phase processed were simulated?

Previous study has found that the absorption of N_2O_5 on aerosols surfaces containing chloride ions leads to the formation of CINO₂ (Finlayson-Pitts et al., 1989). This N_2O_5 uptake process is an irreversible loss: it converts N_2O_5 into stable soluble nitrate and potentially volatile CINO₂, thereby permanently removing gaseous N_2O_5 . CINO₂ will be photolyzed into CI- and NO₂ under sunlight (Chen et al., 2023; Ma et al., 2023; McNamara et al., 2020; Peng et al., 2021). The detailed reactions are as follows:

$$N_2O_5 + Cl^-(aq) \to \varphi ClNO_2 + (2 - \varphi)NO_3^-(aq)$$

$$ClNO_2 \stackrel{k_2}{\to} Cl \cdot + NO_2$$

$$k_2 = j_{ClNO_2}$$

Where φ is the production yield of $ClNO_2$, k_2 is the photolysis rate of ClNO₂ (j_{ClNO_2}) . These details are shown in Supplementary Materials S3.

However, the current chemical mechanism, MCM v3.3.1, lacks these reaction processes, so we added the mechanism of N₂O₅ uptake by aerosols and photolysis of ClNO₂ to MCM v3.3.1 to simulate ClNO₂ and explored its impact on $P(O_3)_{net}$. We set the heterogeneous uptake coefficient of N₂O₅ as 0.02 ($\gamma_{N_2O_5} = 0.02$), and the production yield of $ClNO_2$ as 0.6 ($\varphi = 0.6$). Here the ClNO₂ was derived from model simulations and its related reactions are added into MCM v3.3.1 as:

"% ASA*24175.8*0.02/4:N2O5 = 0.6 CINO2+1.4 PNO3;"

"%J<45>: CINO2 = CI +NO2;"

Where ASA represent the surface area of the ambient aerosols, 24175.8 represent the mean molecular speed of N_2O_5 (cm s⁻¹), 0.6 represent the production yield of ClNO₂, J<45> represent the photolysis rate of ClNO₂. As our previous study has thoroughly described these mechanisms (Zhou et al., 2024a), we have modified the description in lines 199-200 of the modified manuscript:

"..., and Case D_1 extends Case C by adding the N_2O_5 uptake mechanism and Cl· related photochemical reactions. Detailed simulation parameter settings can be found in our previous study (Zhou et al., 2024a) and the supplementary information (Table S3)."

"Table S3. Description of different modelling scenarios and the parameter settings

Case	Description	Parameter settings	references
A	Ambient gases (NO, NO ₂ , SO ₂ , CO, O ₃), HONO, 44 VOCs, meteorological parameters (<i>T</i> , RH, <i>P</i> , BLH), photolysis	O ₃ (0.27 cm s ⁻¹)	(Xue et al., 2014)
В	rates, and O_3 dry deposition Case A with the addition of HO_2 uptake	γ _{HO2} =0.19	(Zhu et al., 2020; Zhou et al., 2021)
С	Case B with the addition of trace gases (NO ₂ , SO ₂ , H ₂ O ₂ , HNO ₃ , PAN, HCHO) dry deposition	$NO_2 \ (0.6 \text{ cm s}^{-1})$ $SO_2 \ (0.8 \text{ cm s}^{-1})$ $H_2O_2 \ (1.2 \text{ cm s}^{-1})$ $HNO_3 \ (4.7 \text{ cm s}^{-1})$ $PAN \ (0.4 \text{ cm s}^{-1})$ $HCHO \ (0.9 \text{ cm s}^{-1})$	(Zhang et al., 2003; Xue et al., 2014)
D_1	Case C with the addition of N_2O_5 non-homogeneous absorption reactions and $CINO_2$ photolysis	$\gamma_{\text{N2O5}}=0.02$ $\varphi_{\text{CINO}_2}=0.6$	(Xue et al., 2014; Badger et al., 2006; Xia et al., 2019; Xia et al., 2020)
D_2	Case D ₁ with increased constraints for acetaldehyde, acrolein, acetone, and		
D_3	butanone Case D ₁ with increased constraints for all measurable OVOCs	Constraints based on measurement data	
D_4	Case D ₃ with increased constraints for all measurable chlorinated VOCs		
E_1	Case D ₁ with overall VOCs concentration in constraints increased		
E_2	Case D_1 with increased concentrations of ethylene and formaldehyde in constraints	Increase based on the correlation between $P(O_3)_{\text{net}}$ Missing and k_{OH} Missing	
E ₃	Case D ₁ with increased formaldehyde concentration in constraints	NOn_IMISSING	

Notes: Parameter values for modelling scenarios from Case A to Case D_1 are set the same as those in Zhou et al. (2024a)."

Minor Points

Please define OFS where first used (abstract, L61)

Thank you for your suggestion. We have added the definition of O₃ formation sensitivity (OFS) in lines 44-49 in the modified manuscript:

"The sensitivity of O₃ formation to its precursors is defined as the O₃ formation sensitivity (OFS), which can be classified into three regimes: NOx-limited, VOC-limited, or mixed sensitivity (Seinfeld & Pandis, 2016; Sillman, 1999). In an NOx-limited regime, the VOC/NOx ratio is high and O₃ production is controlled primarily by changes in NOx. In a VOC-limited regime, the VOC/NOx ratio is low, so O₃ decreases with additional NOx and increases with higher VOCs. In the mixed-sensitivity regime, O₃ rises when either NOx or VOC emissions increase (Wang et al., 2019)."

Accordingly, we used OFS directly in lines 65 in the modified manuscript:

"These gaps lead to systematic biases in the simulated $P(O_3)_{net}$ (Woodward-Massey et al., 2023; Tan et al., 2017; Tan et al., 2019), thereby affecting the accurate determination of OFS."

The related references are added in the references list:

"Seinfeld, J. H. and Pandis, S. N. (Eds. 3): Atmospheric Chemistry and Physics: From Air Pollution to Climate Change, John Wiley & Sons, Hoboken, ISBN 978-1-118-94740-1, 2016.

Sillman, S.: The relation between ozone, NOx and hydrocarbons in urban and polluted rural environments, Atmospheric Environment, 33, 1821–1845, https://doi.org/10.1016/S1352-2310(98)00345-8, 1999.

Wang, P., Chen, Y., Hu, J., Zhang, H., and Ying, Q.: Attribution of tropospheric ozone to NOx and VOC emissions: considering ozone formation in the transition regime, Environmental Science & Technology, 53, 1404–1412, https://doi.org/10.1021/acs.est.8b05981, 2019."

Various places – ppb etc are mixing ratios not concentrations

We changed "concentrations" to "mixing ratios" when describing "ppb" throughout the manuscript.

L165 het loss can be important for HO₂ removal globally – but wont HO2 + NO dominate under the conditions of these BL measurements?

Yes, HO₂+NO dominates under our field measurement conditions, as demonstrated in Fig. S8. However, this dominance refers only to the HO₂ removal rate. For O₃ production, HO₂+NO is a positive source as it

simultaneously produces NO_2 , while HO_2 uptake act as a negative source, similar to other termination reactions (e.g., HO_2+HO_2 , HO_2+RO_2). Therefore, in terms of the negative impact on $P(O_3)_{net}$, the heterogeneous reaction of HO_2 with ambient aerosols is more important than HO_2+NO .

Therefore, we modified the sentence "Although the heterogeneous uptake of HO₂ is not the dominant loss pathway of HO₂, it accounts for approximately 10–40 % of global HO₂ loss (Li et al., 2019); as a termination reaction, its direct negative impact on photochemical O₃ production is non-negligible." in lines 189-191 in the modified manuscript.

References:

Berndt, T., Mentler, B., Scholz, W., Fischer, L., Herrmann, H., Kulmala, M., Hansel A.: 2018. Accretion product formation from Ozonolysis and OH radical reaction of α -Pinene: mechanistic insight and the influence of isoprene and ethylene, Environmental Science & Technology, 52, 11069–11077, doi: 10.1021/acs.est.8b02210, 2018.

Carter, W. P. L., A. Pierce J. A., Luo, D., Malkina, I. L.: Environmental chamber study of maximum incremental reactivities of volatile organic-compounds, Atmospheric Environment, 29, 2499, doi.org/10.1016/1352-2310(95)00149-S, 1995.

Chen, X., Xia, M., Wang, W., Yun, H., Yue, D., and Wang, T.: Fast near-surface CINO₂ production and its impact on O₃ formation during a heavy pollution event in South China, Science of The Total Environment, 858, 159998, doi: 10.1016/j.scitotenv.2022.159998, 2023.

Crounse, J. D., Knap, H. C., Ørnsø, K. B., Jørgensen, S., Paulot, F, Kjaergaard, H. G., and Wennberg, P. O.: Atmospheric Fate of Methacrolein. 1. Peroxy Radical Isomerization Following Addition of OH and O₂. The Journal of Physical Chemistry A, 116, 5756-5762, doi.org/10.1021/jp211560u, 2012.

Finlayson-Pitts, BJ., Ezell, MJ., and Pitts, JN.: Formation of chemically active chlorine compounds by reactions of atmospheric NaCl particles with gaseous N2O5 and CIONO2, Nature, 337, 241-244, doi:10.1038/337241a0, 1989.

Hao, Y., Zhou, J., Zhou, J. P., Wang, Y., Yang, S., Huangfu, Y., Li, X. B., Zhang, C., Liu, A., Wu, Y., Zhou, Y., Yang, S., Peng, Y., Qi, J., He, X., Song, X., Chen, Y., Yuan, B., and Shao, M.: Measuring and modeling investigation of the net photochemical ozone production rate via an improved dual-channel reaction chamber technique, Atmospheric Chemistry and Physics, 23, 9891-9910, 10.5194/acp-23-9891-2023, 2023.

Ma, W., Feng, Z., Zhan, J., Liu, Y., Liu, P., Liu, C., Ma, Q., Yang, K., Wang, Y., He, H., Kulmala, M., Mu, Y., and Liu, J.: Influence of photochemical loss of volatile organic compounds on understanding ozone formation mechanism, Atmospheric Chemistry and Physics, 22, 4841–4851, doi:10.5194/acp.22.4841, 2022.

McNamara, SM., Kolesar, KR., Wang, S., Kirpes, RM., May, NW., Gunsch, MJ., Cook, RD., Fuentes, JD., Hornbrook, RS., Apel, EC., China, S., Laskin, A., Pratt, and Pratt KA.: Observation of road salt aerosol driving inland wintertime atmospheric chlorine chemistry, ACS Central Science, 6, 684-694, doi:10.1021/acscentsci.9b00994, 2020.

Peng, X., Wang, W., Xia, M., Chen, H., Ravishankara, AR., Li, Q., Saiz-Lopez, A., Liu, P., Zhang, F., Zhang, C., Xue, L., Wang, X., George, C., Wang, J., Mu, Y., Chen, J., and Wang, T.: An unexpected large continental source of reactive bromine and chlorine with significant impact on wintertime air quality, National Science Review, 8, 99-109, doi:10.1093/nsr/nwaa304, 2021.

Spindler, G., Hesper, J., Brüggemann, E., Dubois, R., Müller, T., and Herrmann, H.: Wet annular denuder measurements of nitrous acid: laboratory study of the artefact reaction of NO_2 with S(IV) in aqueous solution and comparison with field measurements: Atmospheric Environment, 37, 2643, doi:10.1016/S1352.2310(03)00209.7, 2003.

Stieger, B., Spindler, G., Fahlbusch, B., Müller, K., Grüner, A., Poulain, L., Thöni, L., Seitler, E., Wallasch, M., and Herrmann, H.: Measurements of PM₁₀ ions and trace gases with the online system MARGA at the research station Melpitz in Germany – A five-year study, Journal of Atmospheric Chemistry, 75, 33–70, doi.org/10.1007/s10874-017-9361-0, 2018.

Wang, S., Wu, R., Berndt, T., Ehn, M., and Wang, L.: Formation of highly oxidized radicals and multifunctional products from the atmospheric oxidation of Alkylbenzenes, Environmental Science & Technology, 51, 8442-8449, doi:10.1021/acs.est.7b02374, 2017.

Wu, S., Lee, H. J., Anderson, A., Liu, S., Kuwayama, T., Seinfeld, J. H., and Kleeman, M. J.: Direct measurements of ozone response to emissions perturbations in California, Atmospheric Chemistry and Physics, 22, 4929-4949, oi.org/10.5194/acp-22-4929-2022, 2022.

Xu, Z., Liu, Y., Nie, W., Sun, P., Chi, X., and Ding, A.: Evaluating the measurement interference of wet rotating-denuder – ion chromatography in measuring atmospheric HONO in a highly polluted area: Atmospheric Measurement Techniques, 12, 6737 – 6748, doi:/10.5194/amt.12.6737, 2019.

Zhou, J., Wang, W., Wang, Y., Zhou, Z., Lv, X., Zhong, M., Zhong, B., Deng, M., Jiang, B., and Luo, J.: Intercomparison of measured and modelled photochemical ozone production rates:

Suggestion of chemistry hypothesis regarding unmeasured VOCs, Science of The Total Environment, 951, 175290, doi:10.1016/j.scitotenv.2024.175290, 2024a.

Zhou, J., Wang, W., Wang, Y., Zhou, Z., Lv, X., Zhong, M., Zhong, B., Deng, M., Jiang, B., Luo, J., Cai, J., Li, X.-B., Yuan, B., and Shao, M.: Intercomparison of measured and modelled photochemical ozone production rates: Suggestion of chemistry hypothesis regarding unmeasured VOCs, Science of The Total Environment, 951, 175290, doi:/10.1016/j.scitotenv.2024.175290, 2024b.